Supporting Information

Rational Design and Regulation of Tremella-liked Selenium Doping MoS_2 for Highly Reversible Sodium Storage

Ruiyu Zhu[a], Shiying Li[b], Lixiang Li[b], Chengxin Liu[b], Xiaojie Liu*[,b]

[a]School of Chemistry and Chemical Engineering, Xi'an University of Architecture and Technology, Xi'an 710055, P. R. China

[b]Key Laboratory of Synthetic and Natural Functional Molecule (Ministry of Education), College of Chemistry & Materials Science, Shaanxi Joint Lab of Graphene (NWU), Northwest University, Xi'an 710127, P. R. China

*Corresponding author.

E-mail address: xiaojie.liu@nwu.edu.cn

S1 Experimental section

Synthesis of Mo-glycerate (MoG) nanospheres

All reagents have not undergone any treatment before used. In a typical synthesis of MoG spheres, 8 mL of glycerol and 60 mg of molybdyl acetoacetonate ($MoO_2(acac)_2$) were dispersed in 20 mL of isopropanol (IPA)/ H_2O (V/V = 3:1) under vigorous stirring and then uniform dispersion can obtain after sonicated for 20 min. The mixture was kept at 190 °C for 3 h in 50 mL Teflon- lined stainless steel autoclave. After cooling down, the product was collected after ethanol washing and dried at 80 ºC for 24 h under vacuum.

Synthesis of MoS_2 hollow hierarchical nanospheres

20 mg of dark brownish MoG powder and 40 mg of thiourea were added into 40 mL of solution with ethanol (EtOH)/ H_2O (V/V = 3:1). The mixture solution was then kept at 200 °C for 6 h in 50 mL Teflon-lined stainless-steel autoclave. The product obtained from hydrothermal process were centrifuged, washed and dried.

Synthesis of hollow hierarchical selenium doping MoS_2 nanospheres ($MoS_{2(1-x)}Se_{2x}$)

In a typical process of selenization, the MoS_2 spheres were grinding evenly with selenium powder, and then the mixture was annealed under Ar/ H_2 atmosphere for 2 h at 650 °C. With different molar ratios of MoS_2 precursor and selenium powder, the corresponding products denoted as $MoS_{1.8}Se_{0.2}$, $MoS_{1.5}Se_{0.5}$, MoSSe can be acquired.

Synthesis of $MoS_{2(1-x)}Se_{2x}$ with carbon coating ($MoS_{2(1-x)}Se_{2x}$ @C)

20 mg of $MoS_{2(1-x)}Se_{2x}$ was added into a mixed solution of absolute ethanol (48 ml) and deionized water (2 ml) under vigorously stirring for 5 min. Then, 21 mg of resorcinol and 0.56 ml of formaldehyde were added into the solution, and kept vigorously stirring for 24 h. The product was centrifugated and washed by ethanol for three times, and then dried at 80 °C for 24 h. The final product was obtained after annealed under Ar atmosphere for 2 h at 700 °C with 5 °C min^{-1}.

S2 Materials characterization

The morphologies and microstructures of the as prepared samples were recorded by scanning electron microscopy (SEM, Hitachi SU8010) and transmission electron

microscopy (TEM, JEOL JEM-3010). The crystal structures data of these samples were obtained by Bruker D8 ADVANCE X-ray powder diffraction (Cu Kα radiation). Thermo-gravimetric analysis (TGA; SDTQ600) was performed in air atmosphere within temperature range from room temperature to 800°C with heating rate of 10°C min^{-1}. Raman spectra data were obtained by Nicolet Almega dispersive Raman spectrometer with laser source of 532 nm. Brunauer-Emmett-Teller (BET) surface area and pore size distributions data were obtained by ASAP 2020 PLUS HD88 instrument. X-ray photoelectron spectroscopies (XPS) analyses were performed by PHI5000 Versa Probe III XPS with Al Kα as excitation source.

S3 Electrochemical measurements

The electrochemical performance of CR2025- type coin cells was tested by assembly in a glove box filled with high purity Ar (O_2< 0.1 ppm, H_2O < 0.1 ppm), in which the sample was anode material and sodium foil was counter electrodes. To prepare the working electrodes, a homogenous slurry with composition of the prepared active materials (samples), acetylene black, and carboxy methyl cellulose (CMC) in a weight ratio of 7 : 2 : 1 were grinded carefully in ethanol and water. The as prepared slurries were coated uniformly on nickel foam and dried at 80 °C for 12 h under vacuum. The average active material mass loading on the as prepared anode was 1.0 mg cm^{-2}. The electrolyte was prepared by adding 1 M $NaClO_4$ in solution with ethylene carbonate (EC) /propylene carbonate (PC) (1:1) and 5 wt% fluoroethylene carbonate (FEC) as the additive. The glass fiber film was used as separator between the Na and working electrodes. The cyclic voltammetry (CV) was carried out with scan rate from 0.2 to 2.0 mV s^{-1} to analyze the chemical transformation during the charge/ discharge progress, the electrochemical impedance spectrum (EIS) analysis was performed on a CHI 660D electrochemical workstation.

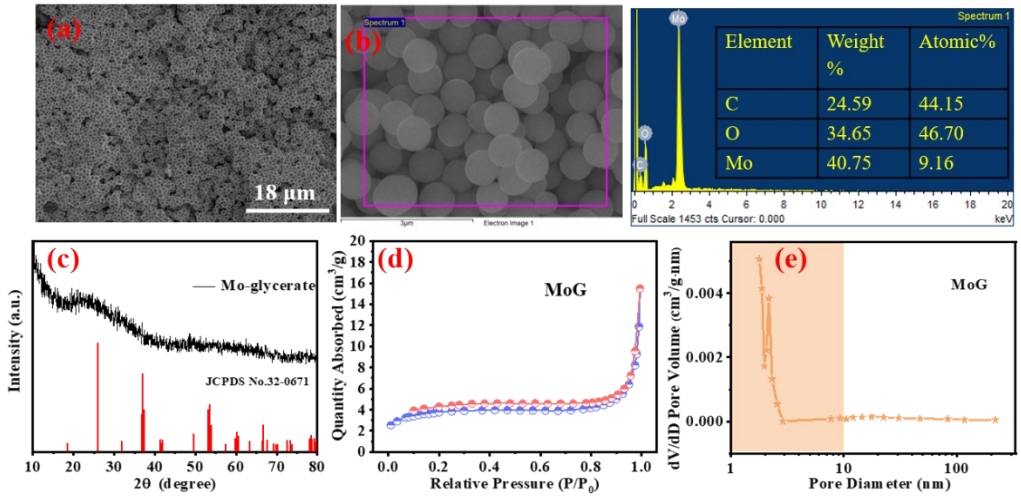

Fig. S1. Morphology/ composition characterization of MoG: (a) SEM. (b) SEM-EDX. (c) XRD pattern. (d,e) Nitrogen adsorption/desorption isotherms matching with BJH pore size distribution.

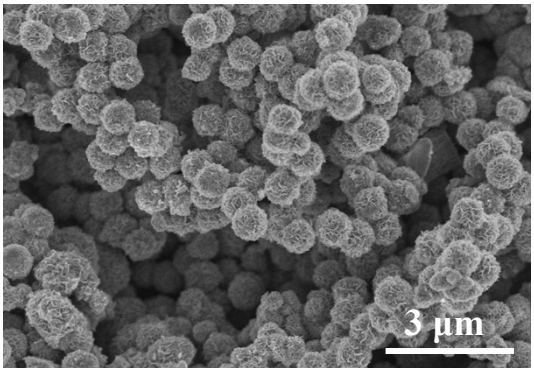

Fig. S2. Low magnification SEM images of MoS_2.

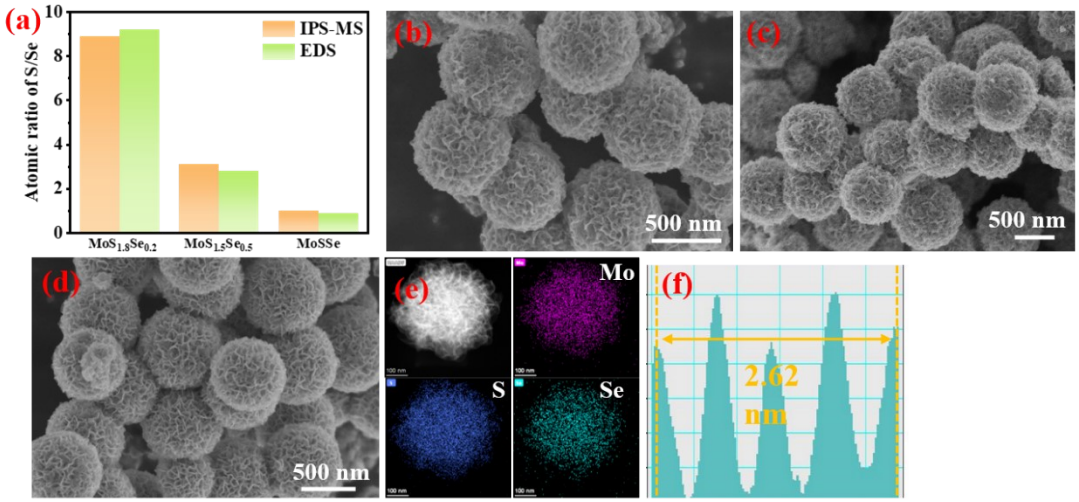

Fig. S3. (a) Atomic ratio of the S/Se from IPS-MS and EDS. SEM images of (b) $MoS_{1.8}Se_{0.2}$, (c) MoSSe, (d) $MoS_{1.5}Se_{0.5}$. (e) Element mapping, (f) Intensity profile across lattice fringes of $MoS_{1.5}Se_{0.5}$.

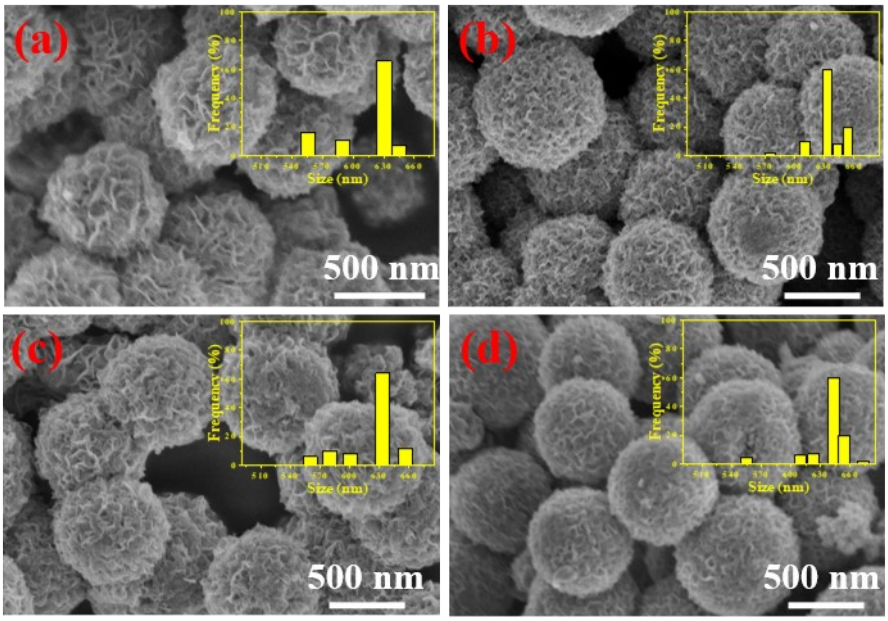

Fig. S4. (a-d) SEM images and particle size distribution of MoS_2@C, $MoS_{1.8}Se_{0.2}$@C, $MoS_{1.5}Se_{0.5}$@C and MoSSe@C.

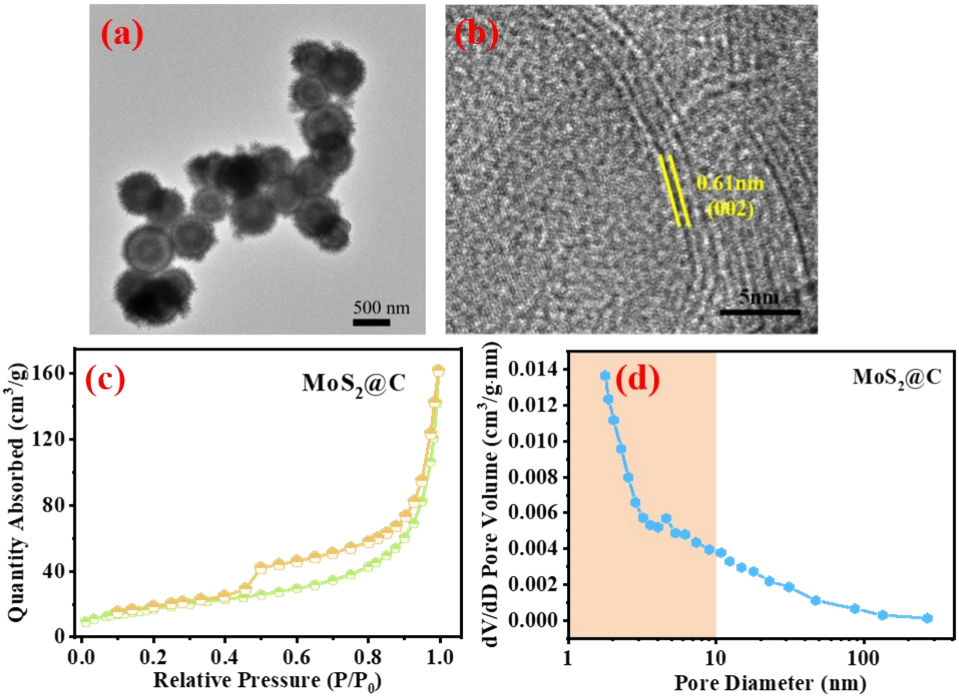

Fig. S5. Morphology/ composition characterization of MoS_2@C: (a) TEM. (b) HRTEM. (c,d) Nitrogen adsorption/desorption isotherms matching with BJH pore size distribution.

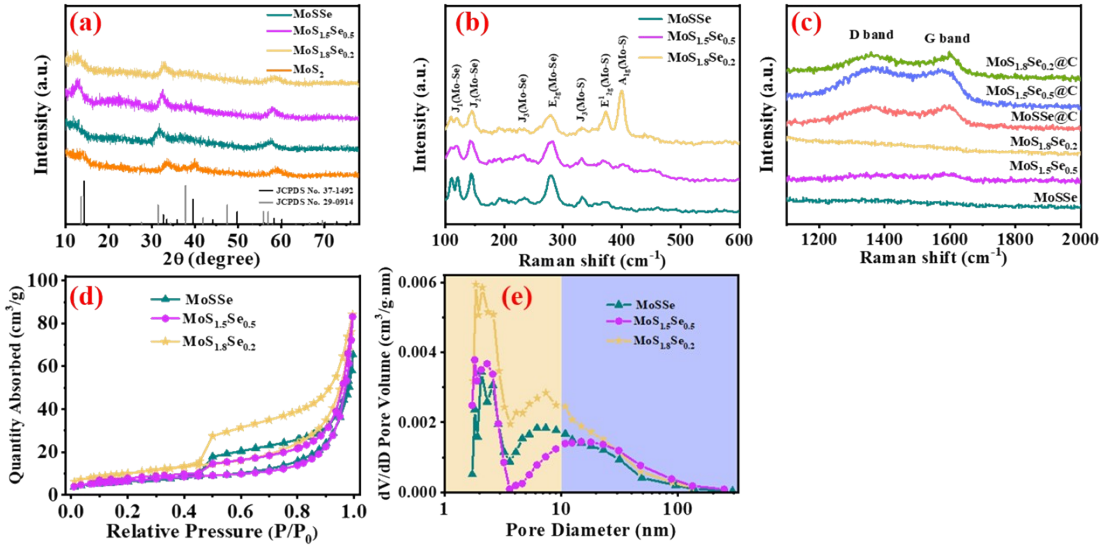

Fig. S6. (a) XRD pattern of MoS_2, $MoS_{1.8}Se_{0.2}$, $MoS_{1.5}Se_{0.5}$ and MoSSe. (b,c) Raman spectra. (d,e) Nitrogen adsorption/desorption isotherms matching with BJH pore size distribution of $MoS_{1.8}Se_{0.2}$, $MoS_{1.5}Se_{0.5}$ and MoSSe.

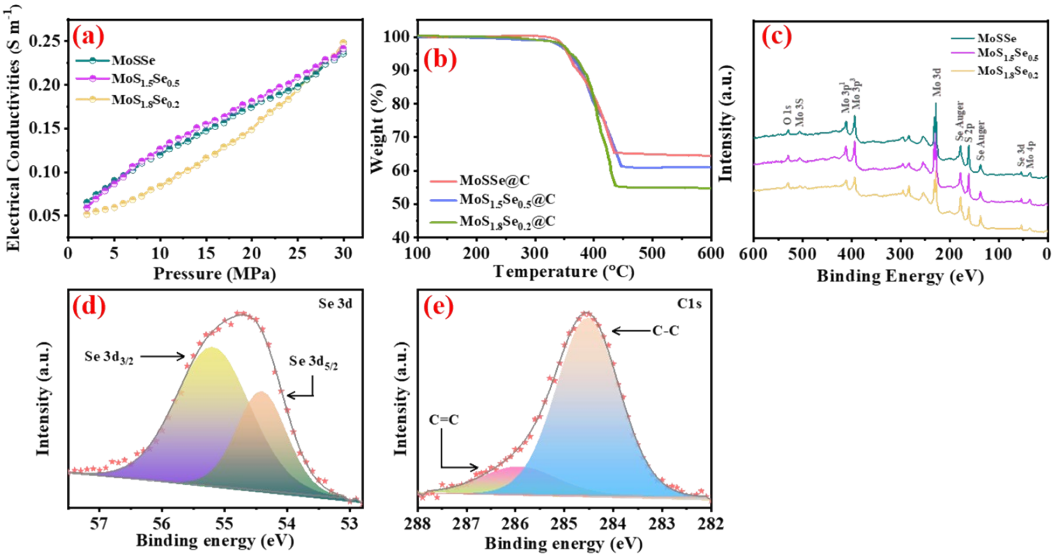

Fig. S7. (a) Electronic conductivities of $MoS_{1.8}Se_{0.2}$, $MoS_{1.5}Se_{0.5}$ and MoSSe. (b) TGA of $MoS_{1.8}Se_{0.2}$@C, $MoS_{1.5}Se_{0.5}$@C and MoSSe@C. (c) XPS full spectra of $MoS_{1.8}Se_{0.2}$, $MoS_{1.5}Se_{0.5}$ and MoSSe. (d) Se 3d and (e) C 1s High- resolution XPS spectra of $MoS_{1.5}Se_{0.5}$@C.

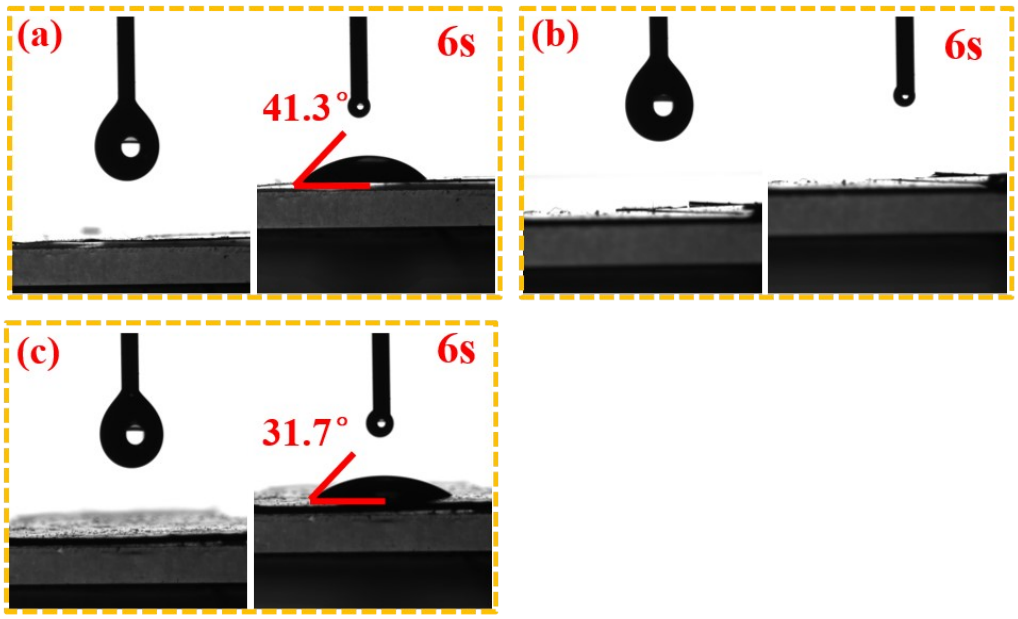

Fig. S8. Surface wet ability for a $NaClO_4$ droplet on (a) $MoS_{1.8}Se_{0.2}$@C, (b) $MoS_{1.5}Se_{0.5}$@C, (c) MoSSe@C surface.

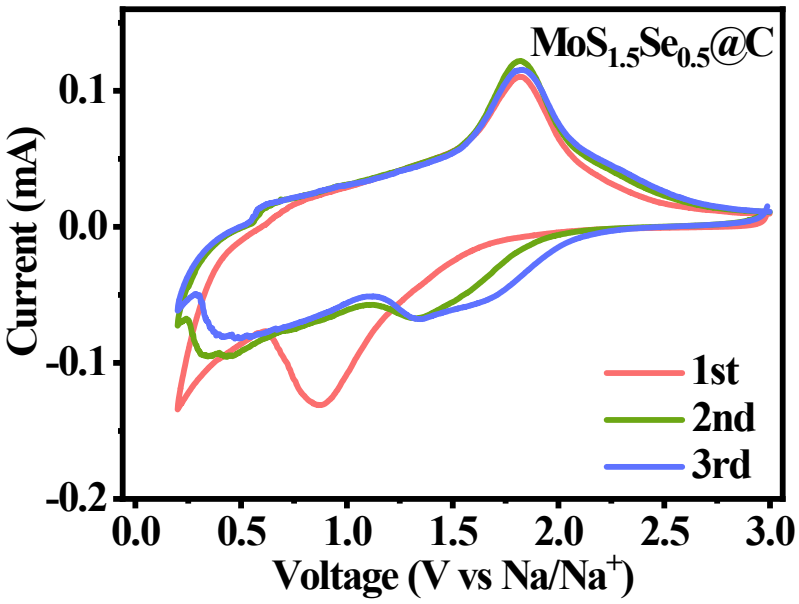

Fig. S9. Initial three cycles CV curves of $MoS_{1.5}Se_{0.5}$@C when the voltage range is set at 0.2- 3V.

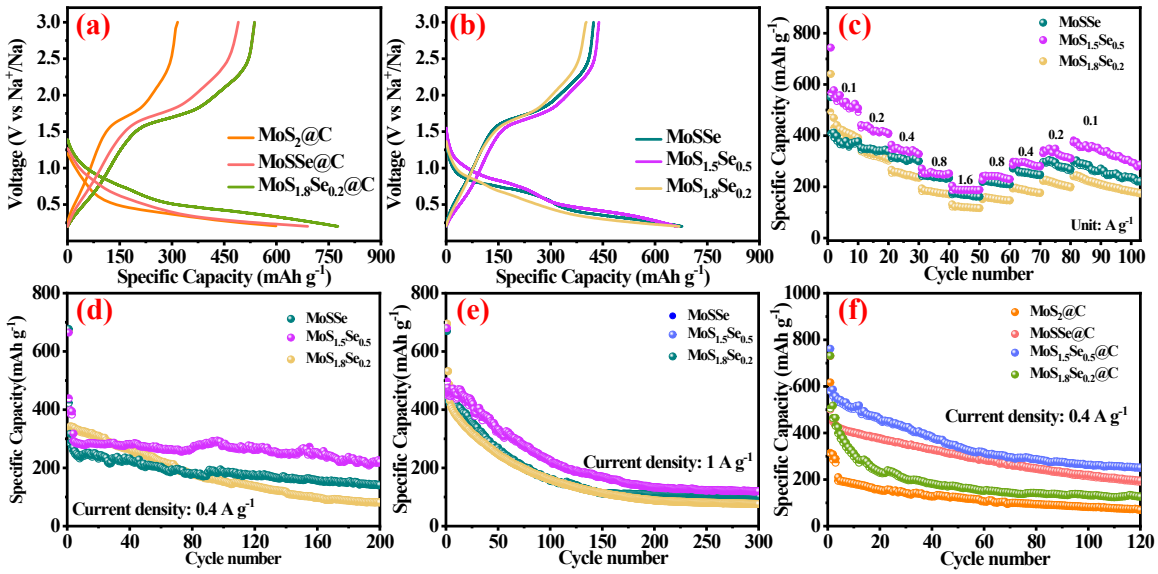

Fig. S10. Initial discharge and charge cycle of (a) MoS_2@C, $MoS_{1.8}Se_{0.2}$@C and MoSSe@C, (b) $MoS_{1.8}Se_{0.2}$, $MoS_{1.5}Se_{0.5}$ and MoSSe. (c) Rate performance, (d,e) Cycles property of $MoS_{1.8}Se_{0.2}$, $MoS_{1.5}Se_{0.5}$ and MoSSe. (f) Cycles property of MoS_2@C, $MoS_{1.8}Se_{0.2}$@C, $MoS_{1.5}Se_{0.5}$@C and MoSSe@C at 0.005-3V.

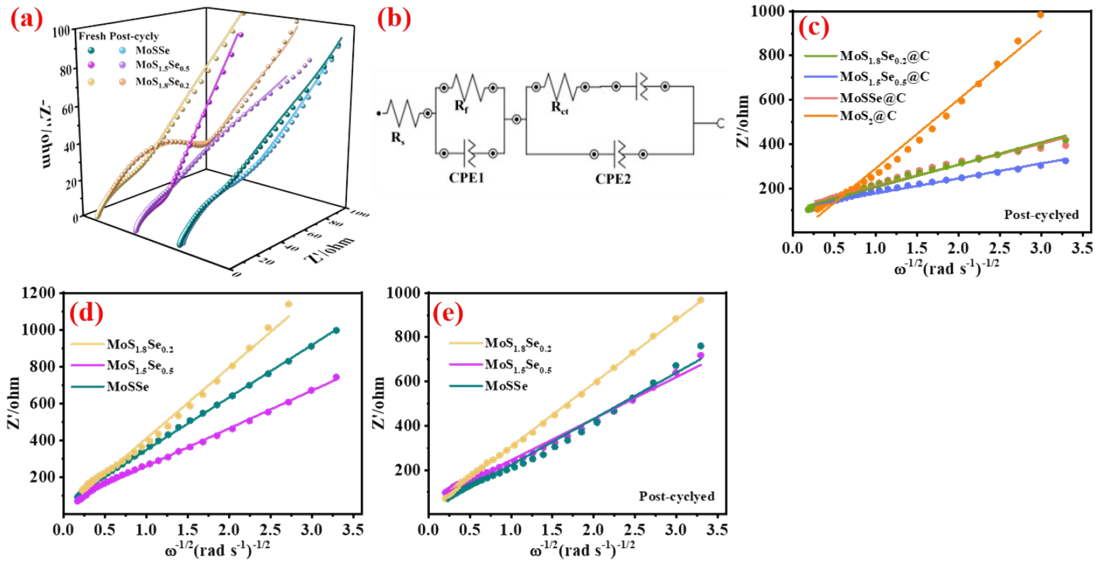

Fig. S11. (a) EIS pattern of fresh and post-cycled $MoS_{1.8}Se_{0.2}$, $MoS_{1.5}Se_{0.5}$ and MoSSe. (b) Equivalent circuit model corresponding with EIS curves. Fitting Z′ and $\omega^{-1/2}$ of (c) post-cycled MoS_2@C, $MoS_{1.8}Se_{0.2}$@C, $MoS_{1.5}Se_{0.5}$@C and MoSSe@C, (d,e) fresh and post-cycled $MoS_{1.8}Se_{0.2}$, $MoS_{1.5}Se_{0.5}$ and MoSSe.

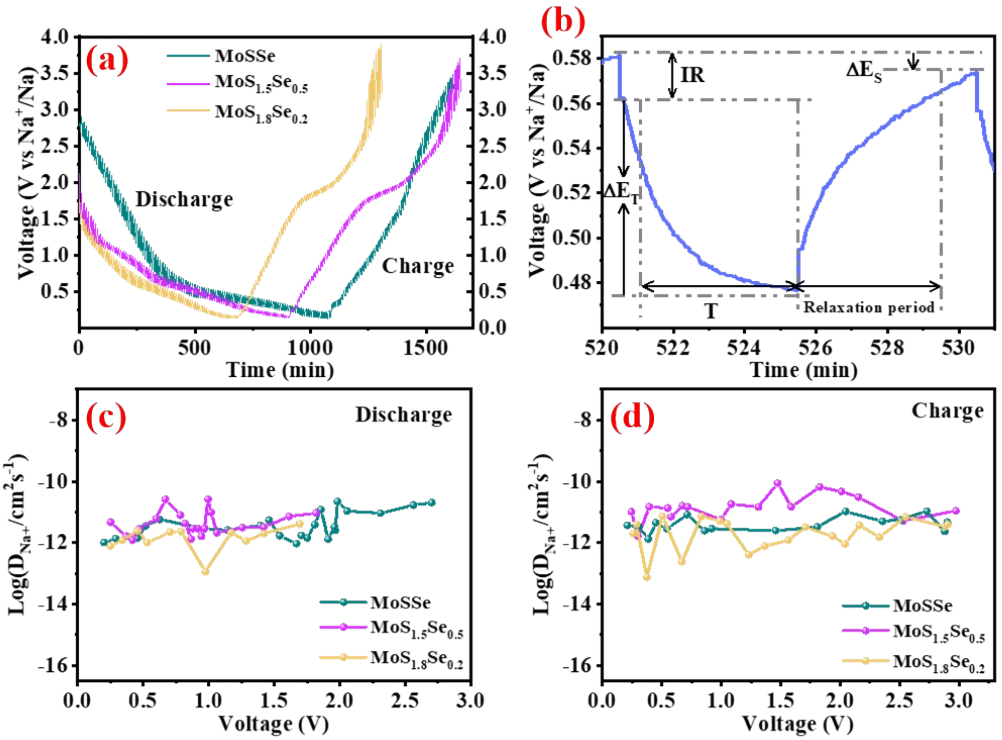

Fig. S12. (a) GITT curves of $MoS_{1.8}Se_{0.2}$, $MoS_{1.5}Se_{0.5}$ and MoSSe. (b) partial enlarged GITT curves. (c,d) Na^+ diffusion coefficient of $MoS_{1.8}Se_{0.2}$, $MoS_{1.5}Se_{0.5}$ and MoSSe.

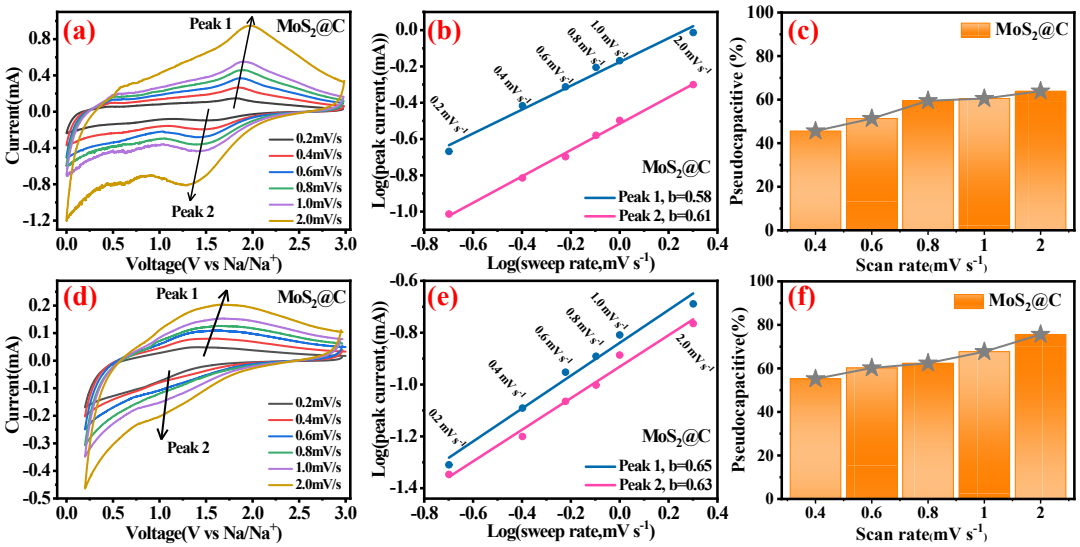

Fig. S13. Electrode kinetics analysis of MoS_2@C: Different scan speeds CV curves, Log i versus log v plots, percent of pseudocapacitance contribution bar chart exhibited during different cutoff voltages of (a-c) 0.005- 3V, (d-f) 0.2- 3V.

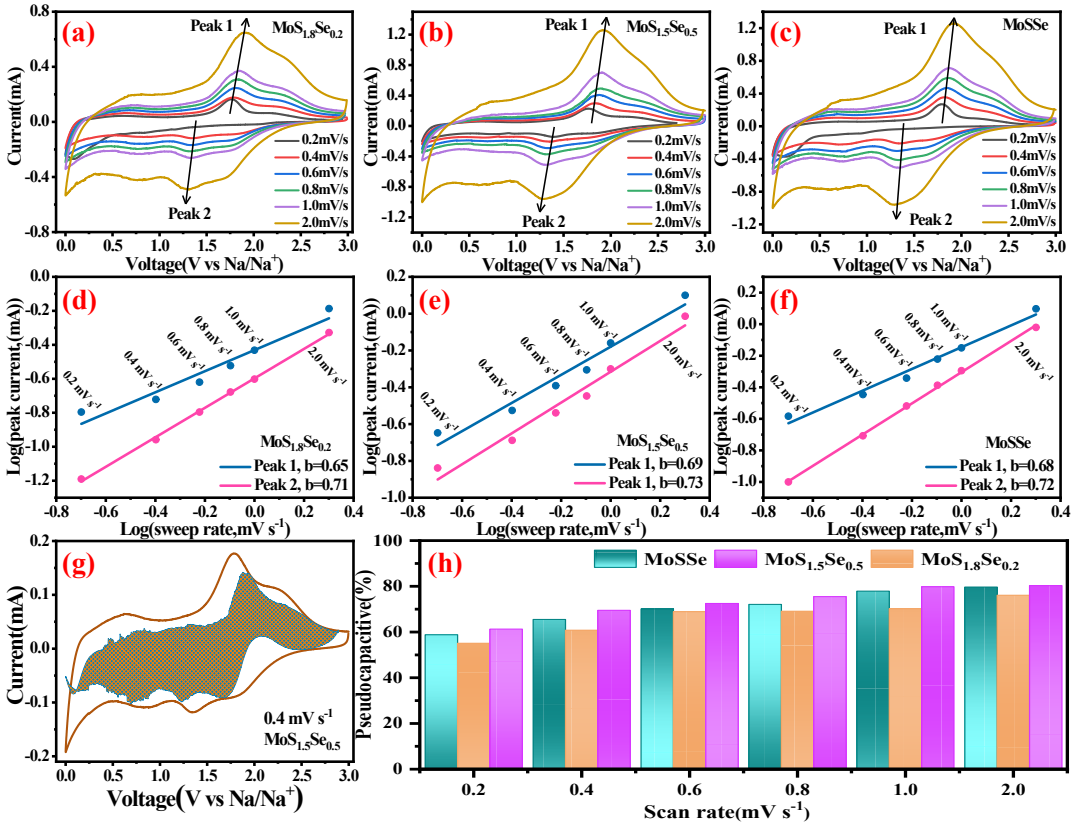

Fig. S14. Electrode kinetics analysis when discharge to 0.005V: (a-c) Different scan speeds CV curves, (d-f) Log i versus log v plots of $MoS_{1.8}Se_{0.2}$, $MoS_{1.5}Se_{0.5}$ and MoSSe. (g) Capacitance control exhibited used shaded region of $MoS_{1.5}Se_{0.5}$. (h) Percent of pseudocapacitance contribution bar chart exhibited of $MoS_{1.8}Se_{0.2}$, $MoS_{1.5}Se_{0.5}$ and MoSSe.

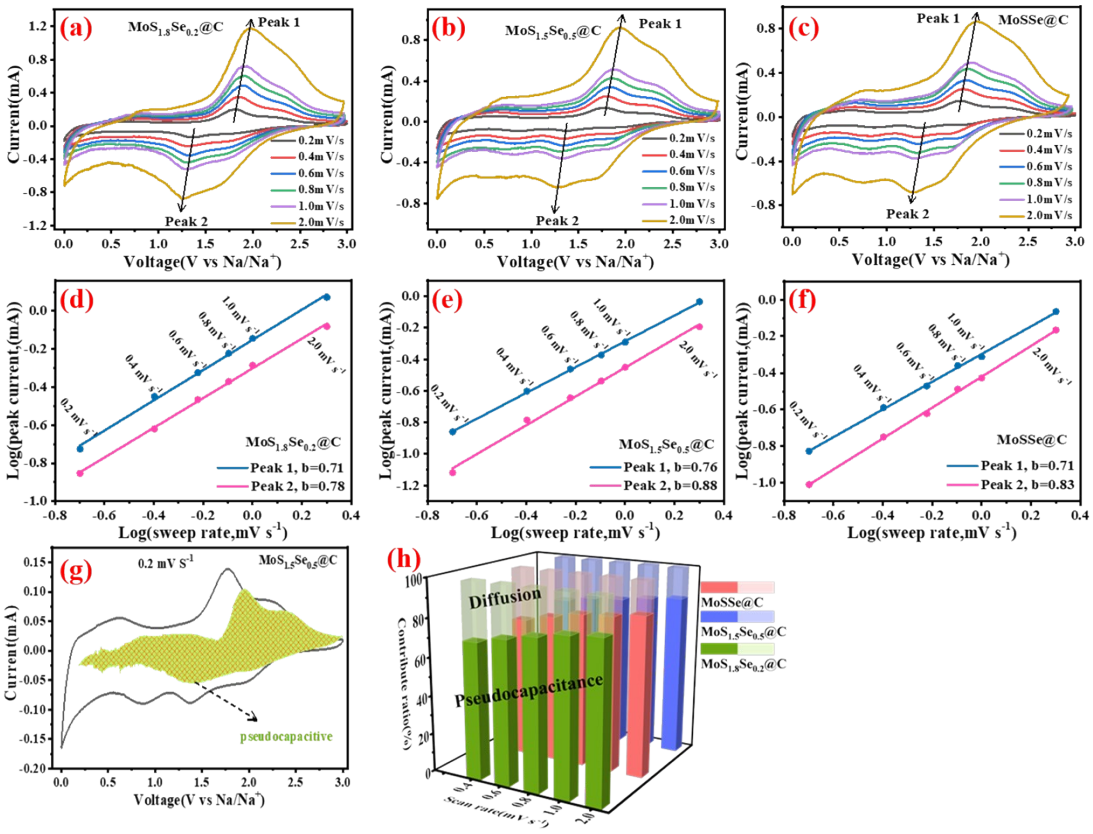

Fig. S15. Electrode kinetics analysis when discharge to 0.005V: (a-c) Different scan speeds CV curves, (d-f) Log i versus log v plots of $MoS_{1.8}Se_{0.2}$@C, $MoS_{1.5}Se_{0.5}$@C and MoSSe@C. (g) Capacitance control exhibited used shaded region of $MoS_{1.5}Se_{0.5}$@C. (h) Percent of pseudocapacitance contribution bar chart exhibited of $MoS_{1.8}Se_{0.2}$@C, $MoS_{1.5}Se_{0.5}$@C and MoSSe@C.

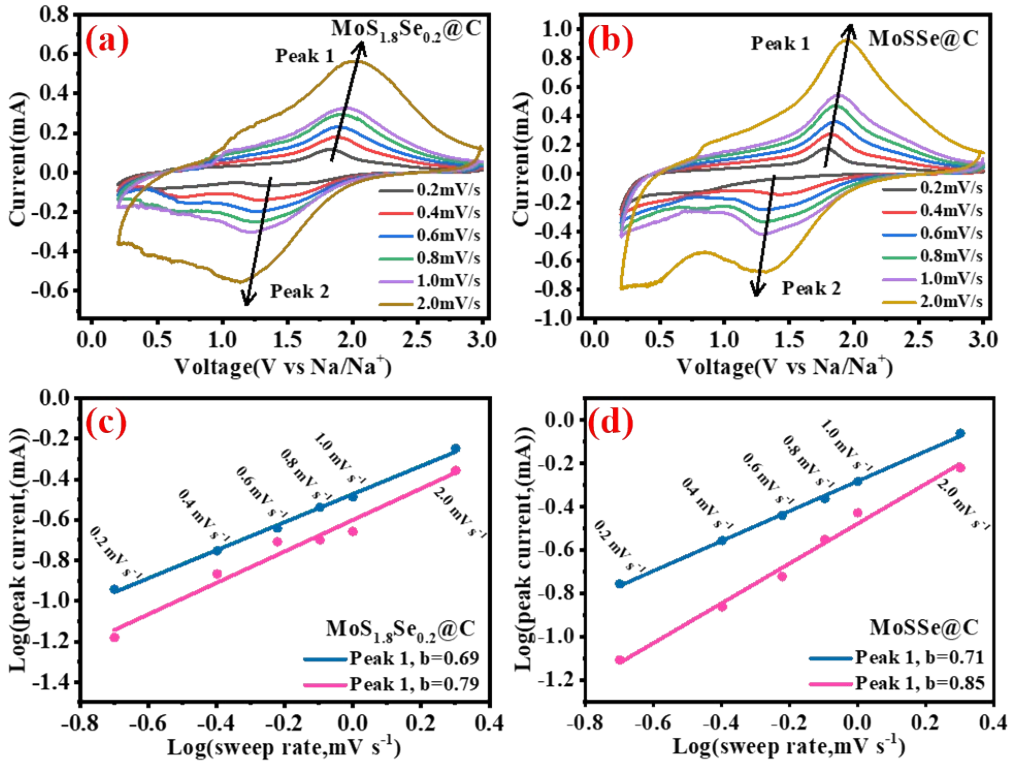

Fig. S16. Electrode kinetics analysis when discharge to 0.2V: (a,b) Different scan speeds CV curves, (c,d) Log i versus log v plots of $MoS_{1.8}Se_{0.2}$@C and MoSSe@C.

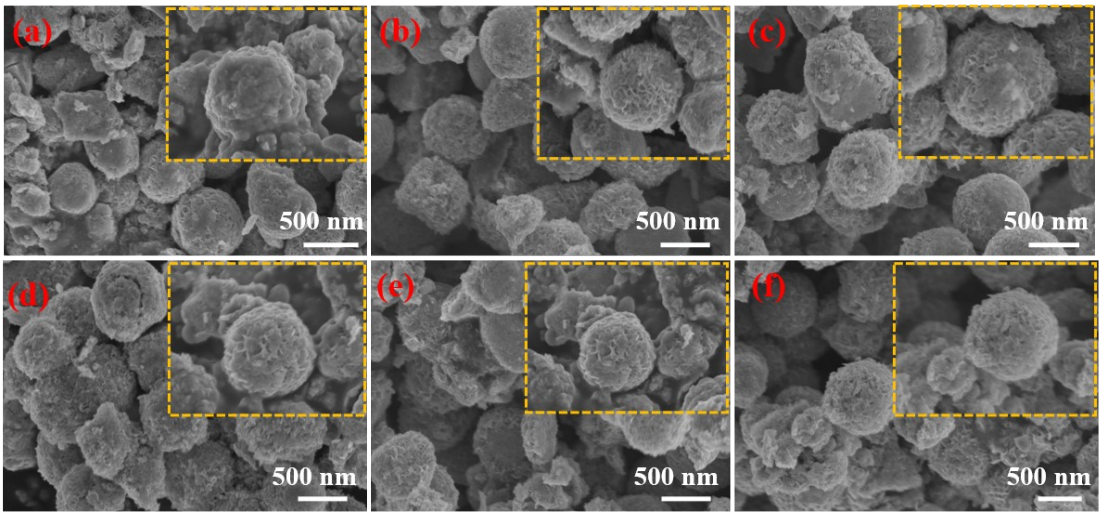

Fig. S17. SEM images of post-cycled (a) MoS_2@C, (b) $MoS_{1.8}Se_{0.2}$, (c) $MoS_{1.5}Se_{0.5}$, (d) MoSSe, (e) $MoS_{1.8}Se_{0.2}$@C, (f) MoSSe@C.

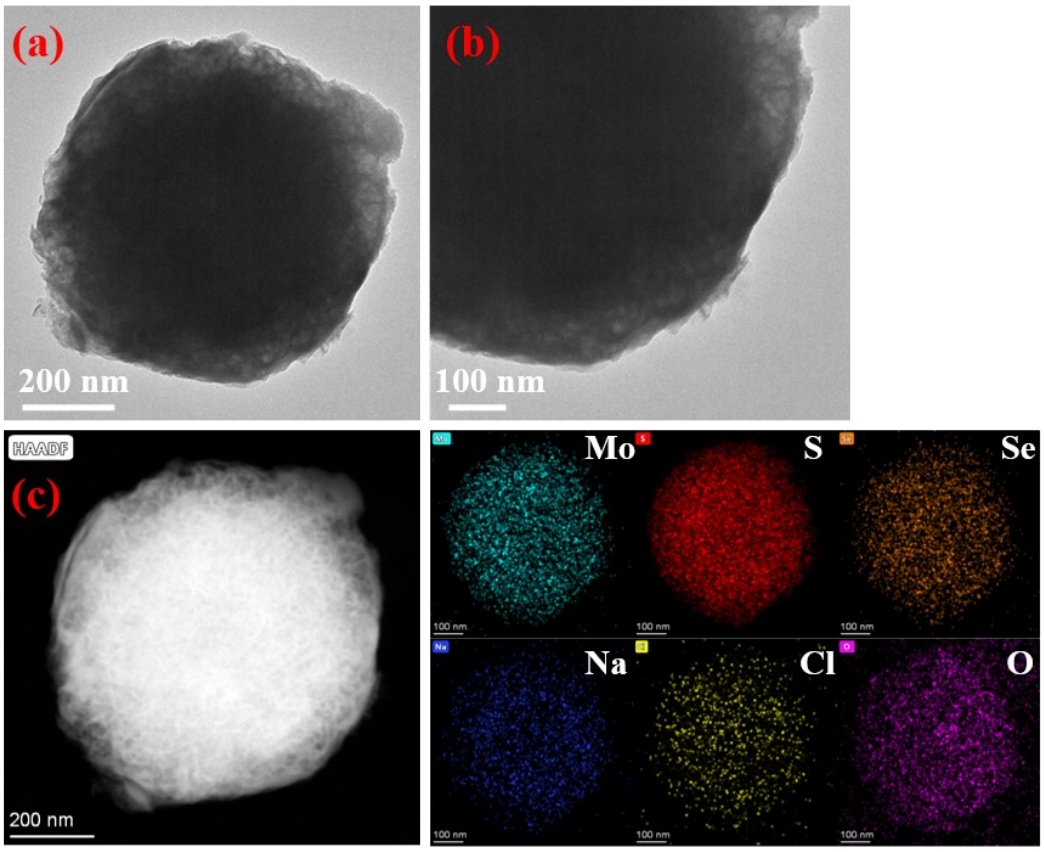

Fig. S18. (a,b) TEM, (c) Element mapping of post-cycled $MoS_{1.5}Se_{0.5}$.

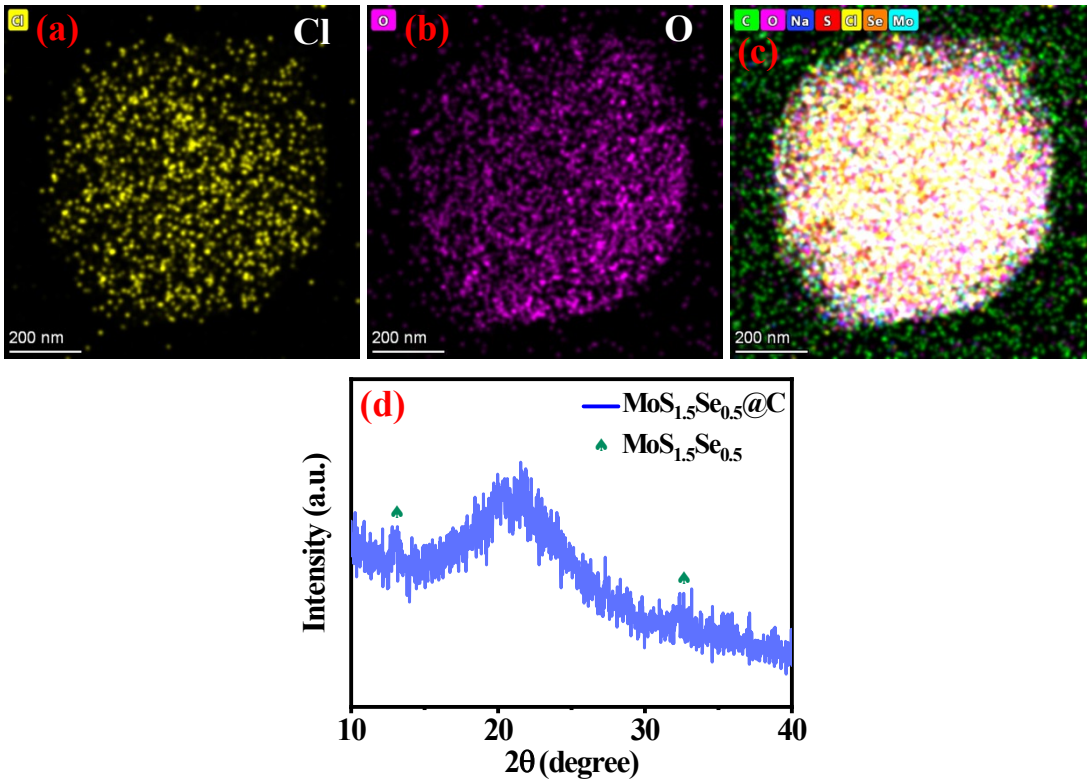

Fig. S19. (a-c) TEM-element mapping of post-cycled $MoS_{1.5}Se_{0.5}$@C. (d) post- cycled XRD pattern of $MoS_{1.5}Se_{0.5}$@C.

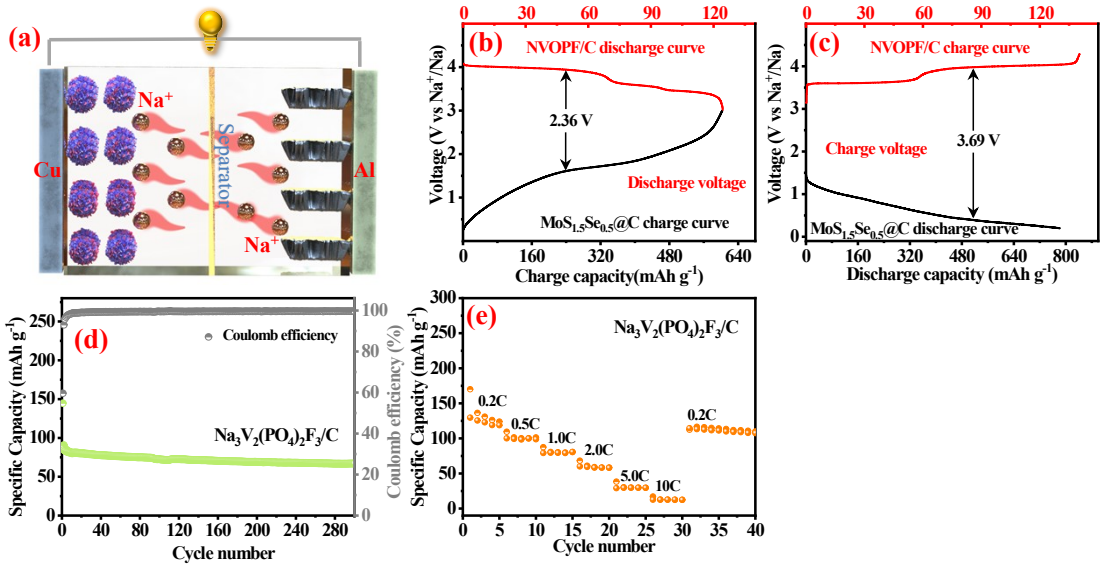

Fig. S20. Electrochemical performance of $MoS_{1.5}Se_{0.5}$@C//$Na_3V_2(PO_4)_2F_3$/C. (a) Working mechanism diagram. (b, c) $Na_3V_2(PO_4)_2F_3$/C discharge/ charge curve combined with $MoS_{1.5}Se_{0.5}$@C charge/ discharge curve. (d, e) the cycle and rate performance of $Na_3V_2(PO_4)_2F_3$/C.

Table S1. Electrochemical performances comparison.

Sample	Current density (A g^{-1})	ICE (%)	Reversible capacity (mAh g^{-1})	Cycle number	Ref.
M-MoS_2@HCS	0.1	34.6	401.3	100	3
MoSSeNSs@NC/hC-NC	0.1	65	453	200	9
Cu_2S@carbon@MoS_2	0.3	65	275	200	10
$MoS_{0.74}Se_{1.26}$/NC	1	64	278	800	19
$MoSe_2$/N-PCD	0.2	70.37	436	500	27
2H-$MoS_{0.2}Se_{1.8}$/rGO	0.5	27	396	100	36
$MoS_{1.5}Se_{0.5}$@C	**1**	**77.3**	**368**	**300**	**This work**

Table S2. Fitted electrochemical impedance value with corresponding Na^+ diffusion coefficients (D_{Na+}) of fresh MoS_2@C, $MoS_{1.8}Se_{0.2}$, $MoS_{1.5}Se_{0.5}$, MoSSe, $MoS_{1.8}Se_{0.2}$@C, $MoS_{1.5}Se_{0.5}$@C and MoSSe@C electrode.

Sample electrode	R_s/Ohm	R_f/Ohm	R_{ct}/Ohm	σ/cm^2 s^{-1}	D_{Na+}/cm s^{-1}
MoS_2@C	7.29	90.1	345	400.2	1.54×10^{-13}
$MoS_{1.8}Se_{0.2}$	5.14	52.9	181	394.7	1.58×10^{-13}
$MoS_{1.5}Se_{0.5}$	4.62	41.9	93.9	210.6	5.56×10^{-13}
MoSSe	5.07	43.5	104	234.3	4.49×10^{-13}
$MoS_{1.8}Se_{0.2}$@C	3.9	28.5	83.7	166.6	8.88×10^{-13}
$MoS_{1.5}Se_{0.5}$@C	3.2	18.9	60.7	65.9	5.57×10^{-12}
MoSSe@C	3.7	21.2	66.1	95.2	2.72×10^{-12}

Table S3. Fitted electrochemical impedance value with corresponding Na^+ diffusion coefficients (D_{Na+}) of post-cycled MoS_2@C, $MoS_{1.8}Se_{0.2}$, $MoS_{1.5}Se_{0.5}$, MoSSe, $MoS_{1.8}Se_{0.2}$@C, $MoS_{1.5}Se_{0.5}$@C and MoSSe@C electrode.

Sample electrode	R_s/Ohm	R_f/Ohm	R_{ct}/Ohm	σ/cm^2 s^{-1}	D_{Na+}/cm s^{-1}
MoS_2@C	6.27	95.3	199	311.2	2.53×10^{-13}
$MoS_{1.8}Se_{0.2}$	5.06	47.6	172	286.5	3.00×10^{-13}
$MoS_{1.5}Se_{0.5}$	4.29	32.4	103	187.7	6.99×10^{-13}
MoSSe	4.49	49.7	137	208.4	5.67×10^{-13}
$MoS_{1.8}Se_{0.2}$@C	3.45	23.4	27	80.6	3.79×10^{-12}
$MoS_{1.5}Se_{0.5}$@C	2.59	15.5	17.9	50.6	9.63×10^{-12}
MoSSe@C	3.33	20.6	21.6	75.2	4.36×10^{-12}

Table S4. The proportion of capacitive contribution when first discharge to 0.2V at different scan rates in MoS_2@C, $MoS_{1.8}Se_{0.2}$@C, $MoS_{1.5}Se_{0.5}$@C and MoSSe@C.

Scan rate (mV s^{-1}) / Sample electrode	0.2/%	0.4/%	0.6/%	0.8/%	1/%	2/%
MoS_2@C	49.2	55.2	60.2	62.4	67.7	75.6
$MoS_{1.8}Se_{0.2}$@C	66.8	74.2	79.9	82.3	83.9	86.9
$MoS_{1.5}Se_{0.5}$@C	71.3	82.9	85.7	87.3	89.4	96.4
MoSSe@C	68.6	76.8	80.2	83.6	85.8	88.8

Table S5. The proportion of capacitive contribution when first discharge to 0.005V at different scan rates in MoS_2@C, $MoS_{1.8}Se_{0.2}$, $MoS_{1.5}Se_{0.5}$, MoSSe, $MoS_{1.8}Se_{0.2}$@C, $MoS_{1.5}Se_{0.5}$@C and MoSSe@C.

Scan rate ($mV\ s^{-1}$) / Sample electrode	0.2/%	0.4/%	0.6/%	0.8/%	1/%	2/%
MoS_2@C	38.9	45.6	51.3	59.5	60.5	63.9
$MoS_{1.8}Se_{0.2}$	55.1	60.8	68.9	69.1	70.2	76.1
$MoS_{1.5}Se_{0.5}$	61.3	69.5	72.5	75.5	79.8	80.3
MoSSe	58.8	65.5	70.1	72.1	77.9	79.7
$MoS_{1.8}Se_{0.2}$@C	62.5	70.6	74.2	77.4	80.3	81.6
$MoS_{1.5}Se_{0.5}$@C	68.8	76.2	78.9	80.1	82.3	83.9
MoSSe@C	65.6	73.2	76.7	79.9	80.9	83.1